Effects of gut microbiota perturbation on Th1- and Th2-biased mice following treatment with Vancomycin

Pratikshya Ray and Palok Aich*

School of Biological Sciences, National Institute of Science Education and Research (NISER), HBNI, P.O. - Bhimpur-Padanpur, Jatni - 752050 Dist. - Khurdha, Odisha, India

*Correspondence:

Dr. Palok Aich

palok.aich@niser.ac.in

Keywords: Microbiota, Vancomycin, Antibiotic, *Akkermansia muciniphila*, Glucose tolerance, Gut permeability, Cecal matter transplantation (CMT)

SRA accession: PRJNA566053

Graphical Abstract

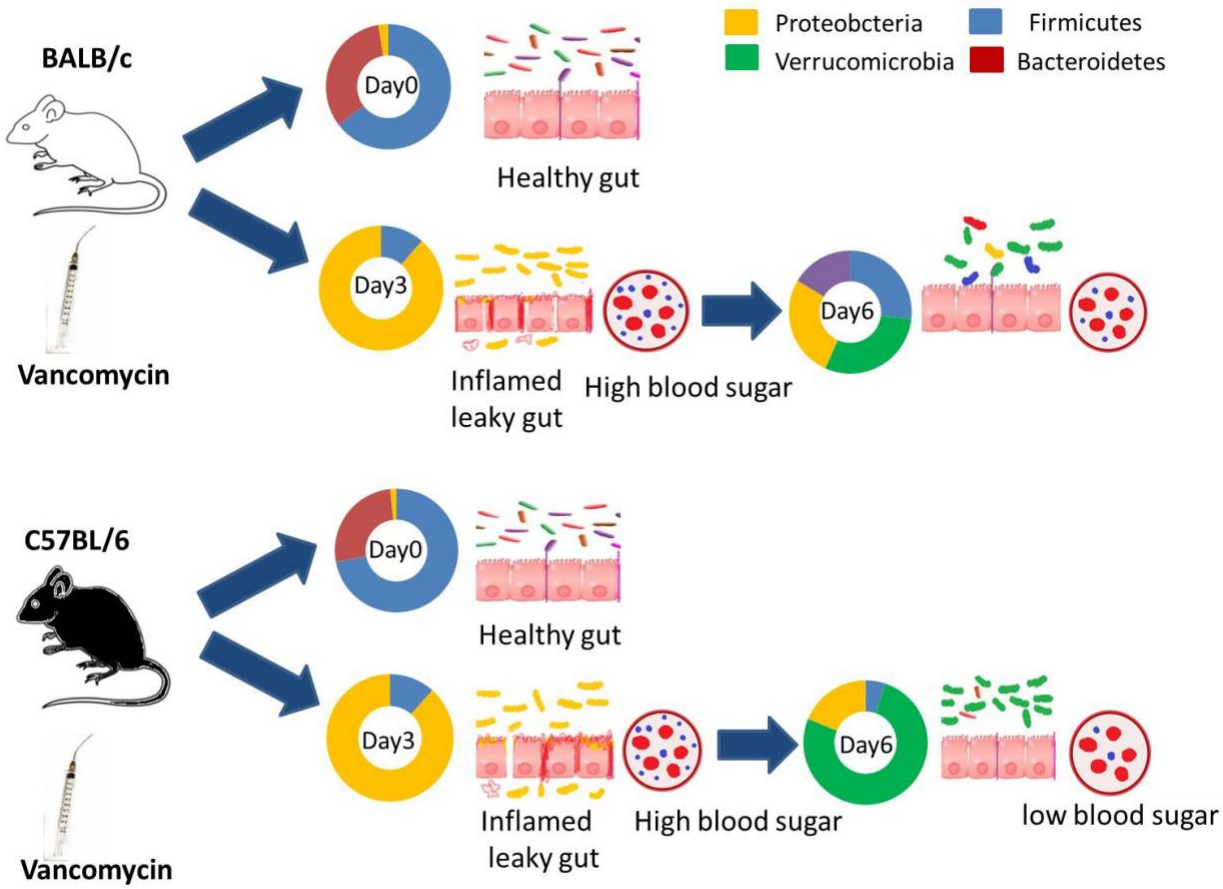

Abstract

The Use and abuse of antibiotics not only cause microbial resistance but also influence the abundance and diversity of gut microbiota. Gut microbiota is a) the largest reservoir of beneficial microbes in mammals and b) plays a major role in maintaining health and homeostasis. An effective way, to understand the role of gut microbiota in maintaining health, is to perturb the gut microbial population. We used the antibiotic, vancomycin, to perturb gut microbiota of Th2- (BALB/c) and Th1- (C57BL/6) biased mice models to understand the altered host response in terms of metabolic and innate immune profile. Results revealed that following treatment with vancomycin until day 4, the abundance of phyla Firmicutes and Bacteroides are reduced while that for Proteobacteria increased in the gut. Results further revealed a significant increase in the phylum Verrucomicrobia from day 5 onwards following treatment with vancomycin. Apparent outcome suggested that the increased Akkermansia led to a) decreased inflammation and b) increased rate of glucose tolerance in the host. The current study showed that initial doses of vancomycin caused adverse effects to the host by increasing pathogenic Proteobacteria (mostly *E.coli* and Shigella) while continued later doses boost certain beneficial microbes from Verrucomicrobia phylum (*A. muciniphila*) in the gut that might provide significant health-related benefits to the host. The effect of elevated abundance of *A. muciniphila* was more prominent in C57BL/6 than BALB/c mice.

Introduction:

Progressive use of antibiotics has raised cautions and warnings regarding antibiotic resistance. The role of commensal microbiota, in maintaining health and perhaps establishing itself as a potential solution in combating antibiotic resistance, is becoming more confluent with newer reports and insights [1–3] Treatment with antibiotics perturb gut microbial milieu [4]. The mammalian

gastrointestinal tract is inhabited by a hundred trillions of highly diverse and complex microbial cells [5]. A large number of these microbes have co-evolved with the host over thousands of years [6]. In fact, these microbes have at least a hundred times more genomic content than the human genome [7, 8]. The abundance and diversity of gut microbiota play significant roles in maintaining various host physiology – for example, harvesting energy [9], maintaining immune homeostasis [10], regulating metabolism [11], and protecting the host against pathogen [12]. While microbiota profile may be diverse and abundant, reports suggested that only a handful of major phyla of gut microbes that include Firmicutes, Bacteroidetes, and Proteobacteria are accounting for at least 90–95% of the gut microbiome. Among these, the anaerobic genera that constitute the majority of gut microbe include Bacteroides, Eubacterium, Clostridium, Ruminococcus, and Faecalibacterium [13].

More reports have started revealing that perturbation of gut microbiota can be used as an effective tool to understand its role in the host. Abundance and diversity of gut microbiota changes with different factors like age [14], diet [15], geography [16, 17], stress [18], pathogen [19], and antibiotics [20]. Since treatment with antibiotics is still the most important and major avenue of dealing with many diseases, it is reported that antibiotics could perturb the general taxonomy of the abundant and diverse gut microbes. Antibiotics are, therefore, being used as one of the most potent agents to study the role of gut microbiota [21]. Because of frequent and long term usage, various commonly used antibiotics can change the composition, diversity, and richness of commensal gut microbiota to result in alteration of different metabolism of the host [22, 23]. The altered microbial profile may lead to different metabolic syndromes like diabetes, obesity, and Inflammatory Bowel Disease [24, 25]. The intensity of the perturbation of commensal microbes,

by antibiotics, depends on different factors like a) the mode of action of a particular antibiotic and b) the presence of various resistant groups of microbes in the gut against the antibiotic [26].

Among various antibiotics, vancomycin is majorly prescribed orally against the infection of two multi-drug resistant strains; i.e., *Clostridium difficile* and *Staphylococcus* [26–28]. Besides the effectiveness of vancomycin in Clostridium Difficile Infection (CDI) patients, it can cause drastic changes in the human gut microbiota by increasing pathogens and by decreasing the commensal healthy microbes [29]. It has also been reported that following treatment with vancomycin in humans for 7 days, genes for oxidative pathways were upregulated and the genes for immune pathways were downregulated [30].

However, the dose and time-dependent effects of vancomycin on gut microbiota are still unknown. The present study focuses on the effect of a clinical dose of vancomycin on mouse gut microbiota and its effect on different physiology of mice. The current study reveals that the changes, that happen in gut microbiota following treatment of mice with vancomycin, are not as evident as reported before. Although initially, vancomycin treatment causes an increase in abundance of specific pathogens and a decrease in native microbes, at the later stage of the treatment, some healthy microbes start appearing and pathogens started declining, which could provide health benefits to the host.

The current laboratory reported earlier the effects of probiotics on the gut microbiota of Th1- and Th2-biased mice [31]. There are also reports that elucidated the intrinsic differences in immune and immune-metabolic responses between C57BL/6 (Th1) and BALB/c (Th2) mice [32, 33]. We reported the differences in gut microbiota from phylum to genus between the two strains (Th1- and Th2-biased) of mice [34]. In the current study, we reported the role of vancomycin on gut microbiota in Th1- and Th2-biased mice. The microbiota present in the gastrointestinal tract is

important for the development of a mature immune system of the host [35]. Reports revealed that the gut microbiota influenced the immune system of the host through the interaction of their molecular patterns (lipopolysaccharide, peptidoglycan) with toll-like receptors (TLR4, TLR2) present in the epithelial cell of the gut. The receptor-ligand interactions produced various cytokines and chemokines for downstream immune regulation [36, 37]. In this study, following vancomycin treatment, we observed and correlated the kinetics of immunological changes of the host at both transcriptional and protein level with metagenomic changes in the gut of C57BL/6 and BALB/c mice.

Microbiota present in the gut can control the host metabolism of major nutrients like carbohydrates, amino acids, fatty acids, and vitamins. Studies reported that some microbes could convert complex carbohydrates into short-chain fatty acids (SCFAs) like acetate, propionate, and butyrate. These SCFAs play important roles in regulating inflammatory response and metabolism of the host by binding to free fatty acid receptors (e.g. FFAR2/3) present in the intestinal epithelial cells, immune cells and adipocytes [36].

Intestinal epithelium acts as a barrier to the entry of different pathogens, inflammatory molecules and toxins into the mucosal tissue [37]. The commensal microbes present on intestinal epithelial cells maintain the integrity of gut permeability by controlling the expression of various tight junction proteins such as by occludin, claudin, and mucin [38]. The defects in barrier due to perturbation of gut microbiota lead to different metabolic diseases like Inflammatory Bowel Disease, obesity, and diabetes [24–26]. The current report reveals that the variation in the abundance and diversity of different groups of microbes, in Th1- and Th2-biased mice, could differentially regulate the gut barrier integrity, host inflammation, and glucose tolerance.

Material and methods:

Animals Used in the study: All mice of the same strain used in the present study were co-housed in polysulfone cage, and corncob was used as bedding material. Food and water were provided as and when required. Animals were co-housed in a pathogen-free environment with a 12h light-dark cycle at temperature 24 ± 3° with the humidity around 55%. The guidelines for animal usage was as per CPCSEA (Committee for the Purpose of Control and Supervision of Experiments on Animals, Govt. of India). All protocols were approved by the Institute Animal Ethics Committee constituted by CPCSEA (Reg. No.- 1643/GO/a/12/CPCSEA). Two mice strains C57BL/6 (Th1) and BALB/c (Th2) of 6-8 weeks of age were used in the present study. Unless otherwise stated, we used at least 3 mice per treatment condition per time point.

Antibiotic treatment: Both Th1-(C57BL/6) and Th2- (BALB/c) biased mice were treated (n=3 per group) with vancomycin (Cat#11465492) twice daily for 6 consecutive days. Vancomycin was administered by oral gavaging at 50 mg per kg of body weight. The dosage was selected as per previous reports and FDA guideline [39, 40].

Mice treatment and sample collection: Mice were separated into two different groups: Control (untreated) and Treatment (groups that were treated with vancomycin). Each day of experiment for 6 days, time-matched control (n=3) and treated (n=3) mice were euthanized by cervical dislocation. The tissue samples were collected from duodenum, jejunum, ileum, colon, serum and cecal materials were isolated from each mouse following the protocols described elsewhere. Tissue samples, not used immediately, were stored either by snap freezing for protein analysis or in RNAlater for RNA analysis until further used [41, 42].

Cecal Sample plating: Cecal sample was collected from both strains of mice on day 4 following treatment with vancomycin. 50 mg of each sample was dissolved in 1ml of deionized MilliQ water

and plated at a dilution of 10_4 fold on Salmonella-Shigella specific media and EMB (Eosin methylene blue agar plate) agar plate [43].

RNA extraction: RNA was extracted from the gut wall tissue by using RNeasy mini kit (Cat# 74104, Qiagen, India) following the manufacturer's protocol. 20-23 mg of tissue was processed using liquid nitrogen followed homogenization in 700 µl of RLT buffer. An equal volume of 70% ethanol was added and mixed well. The solution was centrifuged at 13,000 rpm for 5 minutes at room temperature. The clear solution containing lysate was passed through RNeasy mini column (Qiagen, Germany), which leads to the binding of RNA to the column. The column was washed using 700 µl RW1 buffer and next with 500 µl of RPE buffer. RNA was eluted using 30 µl of nuclease-free water. RNA was quantified using NanoDrop 2000 (ThermoFisher Scientific, Columbus, OH, USA).

cDNA preparation: cDNA was synthesized by using AffinityScript One-Step RT-PCR Kit (Cat# 600559, Agilent, Santa Clara, CA, USA). RNA was mixed with random nonamer primer, Taq polymerase, and NT buffer. The mixture was kept at 45 °C for 30 min for the synthesis of cDNA and temperature increased to 92 °C for deactivating the enzyme.

Real-time PCR (qRT-PCR): Real-time PCR performed in 96-well plate, using 25 ng cDNA as template, 1 µM of each of forward (_F) and reverse (_R) primers for genes mentioned in Table 2, SYBR green master mix (Cat#A6002, Promega, Madison, WI, USA), and nuclease-free water. qRT-PCR was performed in Quantstudio 7 (Thermo Fisher Scientific, Columbus, OH, USA). All values were normalized with cycle threshold (Ct) value of GAPDH (internal control) and fold change of the desired gene was calculated with respect to the control C_t-value as mentioned elsewhere [44, 45].

Cytokine Analysis at protein level

Colon tissues were collected from mice on day 0 (untreated control) and on days 3 and 6 following treatment with vancomycin. After washing the colon tissues thoroughly, lysis buffer (Tris-hydrochloric acid, sodium chloride, and Triton X-100 in distilled water) containing 1X protease inhibitor cocktail (PIC) (Cat#ML051, Himedia, India) was used to churn the tissue [40]. The supernatant was collected following centrifuging the churned mixture at 20,000g for 20 minutes. ELISA (BD Biosciences, San Diego, CA, USA) was performed using the manufacturer's protocol for TNFα (Cat#560478) and IL10 (Cat#555252) expression [40]. Protein concentration was normalized through Bradford assay (BD Biosciences, San Diego, CA, USA). The absorbance was taken using Multiskan Go (Thermo Fisher Scientific, Columbus, OH, USA).

Genomic DNA extraction: Cecal sample was collected from mice of both strains and gDNA was extracted using the phenol-chloroform method. 150-200 mg of cecal sample was used to homogenize using 1ml of 1X PBS and centrifuged at 6700g for 10 minutes. The precipitate was lysed by homogenizing it in 1ml of lysis buffer (containing Tris-HCl 0.1M, EDTA 20 mM, NaCl 100 mM, 4% SDS (at pH 8) and thereafter heating it at 80 °C for 45min. Lipid and protein were removed from the supernatant using an equal volume of phenol-chloroform, this process was repeated until the aqueous phase becomes colorless. DNA was precipitated overnight at -20 °C with 3 volumes of absolute chilled ethanol. Finally, it was washed with 500 µl of 70% chilled ethanol and briefly air-dried. The gDNA was dissolved in nuclease-free water and quantified using NanoDrop 2000.

Serum collection: Mice were anesthetized and blood was collected by cardiac puncture. Blood was kept on ice for 30 mins and centrifuged at 1700 RCF for 15 min at 4°C, and serum was collected for further analysis. If required, serum was stored at -80°C till further used.

16S-rRNA sequencing (V3-V4 Metagenomics):

Using cecal DNA samples, V3-V4 regions of 16S rRNA gene was amplified. For this amplification, V3F (Forward primer): 5'-CCTACGGGNBGCASCAG-3' and V4R (Reverse primer): 5'-GACTACNVGGGTATCTAATCC-3' primer pair was used. In Illumina Miseq platform, amplicons are sequenced using paired-end (250bpX2) with a sequencing depth of 500823.1 ± 117098 reads (mean ± SD). Base composition, quality and GC content of fastq sequence were checked. More than 90% of the sequences had Phred quality score above 30 and GC content nearly 40-60%. Conserved regions from the paired-end reads were removed. Using FLASH program, a consensus V3-V4 region sequence was constructed by removing unwanted sequences [46, 47]. Pre-processed reads from all the samples were pooled and clustered into Operational Taxonomic Units (OTUs) by using de novo clustering method based on their sequence similarity using UCLUST program. QIIME was used for the OTU generation and taxonomic mapping [48, 49]. A representative sequence was identified for each OTU and aligned against the Greengenes core set of sequences using PyNAST program [50–53]. Alignment of these representative sequences against reference chimeric data sets was done and the RDP classifier against the SILVA database was used for taxonomic classification to get rid of hybrid sequences.

CMT (cecal microbiota transplantation): Cecal sample was collected from sixth-day vancomycin treated mice and diluted with PBS (1gm/10ml) to make stock. 400 µl of the stock of cecal material was orally gavaged to each of third-day vancomycin treated mice.

Glucose tolerance test (GTT): GTT was assayed on days 0, 3 and 6 following treatment of both types of mice with vancomycin. Following 6h of starvation of mice from each treatment group, fasting blood glucose level (considered as control glucose level at 0 minute) was measured by a glucometer by tail vein bleeding. Mice, fasted for 6h, were orally gavaged with glucose at a dose of 1 mg/g body weight of mouse. Blood glucose levels were measured at intervals of 15-, 30-, 60-

and 90-minutes post-glucose gavaging by using blood glucose monitoring system (ACCU-CHEK Active, Roche Diabetes Care GmbH, Mannheim, Germany).

The same procedure was adopted for oral glucose tolerance test was done for third day CMT recipient mice following 24h of CMT procedure.

Sample preparation and NMR data acquisition for metabolomics study

Serum was isolated from blood of vancomycin treated and control mice as described before. Proteins in the serum were removed by passing it through pre-rinsed (7 times washed) Amicon Ultra-2ml 3000 MWCO (Merck Millipore, USA) column. Centrifugation was done at 4°C at 12,000g. Total of 700 µL solution (containing serum sample, D_2O, pH maintenance buffer and DSS) was taken in 5 mm Shigemi tubes. NMR for all samples were performed at 298K on a Bruker 9.4 T (400 MHz) AVANCE-III Nanobay liquid-state NMR spectrometer equipped with 5 mm broadband (BBO) probe. Pre-saturation technique was used with a moderate relaxation delay of 5 seconds to ensure complete water saturation. Offset optimization was performed using a real-time 'gs' mode for each sample. Topspin 2.1 was used to record and process the acquired spectra.

Metabolomic Analysis of NMR data

ChenomX (Canada) was used for the analysis of NMR data. The Bayesian approach is used to derive metabolite concentration in serum. The phase and baseline of raw spectrum were corrected and concentrations of metabolites were obtained through a profiler using Metaboanalyst [54–57]. To normalize the data acroos the study, the samples were log-transformed and compared with the control sample. Relative fold-change values in metabolite expression analysis was performed for each treated samples with respect to the untreated time-matched control. More than 2-Fold change values (above or below reference value) with $p \leq 0.05$ were considered for further analysis.

Calculation of Cecal index: The body weight of each individual mouse was measured and recorded. The whole cecal content was collected in a microfuge tube and weighed for each individual mouse. The cecal index was measured by taking the ratio of cecal content to the bodyweight of respective mouse and used by normalizing the data with respect to the average bodyweight of mouse used [58].

Gut permeability test by FITC dextran: Mice used for this experiment were water-starved overnight. Next day morning, FITC-dextran (Cat#F7250, Sigma-Aldrich, Missouri, US) at a concentration of 100 mg/ml was dissolved in PBS and oral gavaged. After 4h, mice were anesthetized by isoflurane inhalation and the blood was collected by cardiac puncture. Serum was collected from blood and abundance of FITC in serum was measured by spectro-fluorometry with an excitation wavelength of 485 nm (20 nm bandwidth) and emission of 528 nm (20 nm bandwidth) [59].

Endotoxin detection assay from serum: Mice were sacrificed on days 0, 3 and 6 following treatment of mice with vancomycin and blood was collected by cardiac puncture in an endotoxin-free vial. Toxinsensor chromogenic LAL endotoxin assay kit from GeneScript (Cat#L00350, Piscataway, NJ, USA) was used for detecting endotoxin level in the serum of mice using the manufacturer's protocol [60].

Acetate detection assay in serum: Acetate level was measured in the serum samples of untreated (control day 0) and day 6 following treatment of BALB/c and C57BL/6 mice with vancomycin by using acetate colorimetric assay kit (EOAC-100, San Francisco, USA). Both control and treated mice were anesthetized and blood was collected through cardiac puncture. Blood was kept on ice for 30 mins followed by centrifugation at 1700 rpm for 15 min at 4 °C. The supernatant was

collected and 10 µl of serum from each sample was used to detect acetate level using substrate-enzyme coupled colorimetric reaction assayed by absorbance at 570 nm.

Hormonal assay: Leptin (Cat# ELM-Leptin), and Insulin (Cat# ELM-Insulin) hormone levels were assayed in serum samples. PYY (Cat# EIAM-PYY) was assayed in the gut tissue samples by using Raybiotech mouse hormonal assay kit (Norcross, Georgia, USA).

Statistical Analysis

All the graphs were plotted using GraphPad Prism version 7.0. Statistical package in Prism was used for statistical analysis for the data to perform 't'-test (to compare any 2 data sets) or ANOVA (to compare more than two datasets) as described in the text.

Result:

Vancomycin treatment alters the abundance and diversity of gut microbiota

Two important parameters, in microbiota research, are abundance and diversity that account for various physiological functions of the microbes. Metagenomic (16S rRNA) analysis of the cecal content in vancomycin treated mice showed a decrease in major phyla of bacteria like Firmicutes and Bacteroidetes and an increase in proteobacteria level (Figs. 1(b) and 1(d)) compared to untreated time-matched mice (Figs. 1(a) and 1(c)). Comparing the phyla of untreated control samples (Figs. 1(a) and 1(c)) with vancomycin treated samples (Figs 1(b) and 1(d)) for both mouse strains, the results revealed that Proteobacteria level in vancomycin treated mice increased from 1-2% (with respect to control group) to 90% (on day 4 following treatment with vancomycin). On the contrary, Firmicutes level decreased from 70-80% (untreated control group) (798923 of total 1125245 OTU) to below 10% (fourth day following treatment with vancomycin) (17357 of total 347154 OTU) and Bacteroidetes level from 25-30 % (untreated group) (281311 of total 1125245

OTU) to 1% (fourth day following treatment with vancomycin) (3432 of total 347154 OTU) (Figs 1(b) and 1(d)).

In addition, we further determined the diversity of the cecal microbiota. Shannon equitability index for diversity at the phylum level showed a decrease in diversity up to the fifth day of treatment in BALB/c (Fig.1(e)) and fourth day of treatment in C57BL/6 mice (Fig.1(f)). Diversity increased on day 6 for BALB/c and day 5 for C57BL/6 following treatment with vancomycin. Changes in the abundance and diversity in cecal microbiota opened up avenues for newer explorations some of which are reported here later.

Comparative analysis of time-dependent changes of genus level data in time matched untreated controls (Fig. 2(a) and Fig. 2(c)) with vancomycin treated BALB/c and C57BL/6 (Figs 2(b) and 2(d)) corroborated with phylum level results (Fig. 1). When Shannon equitability index for measuring diversity between phylum and genus level data were compared, it was observed that the trend of the data at both levels until day 5 were similar but absolute values were different (Table 1). Day 6 values for phylum and genus were similar for either BALB/c or C57BL/6 (Table 1). The data was further validated by plating the cecal samples of the day 4 vancomycin treated mice on specific media such as salmonella-shigella specific agar and EMB agar plate. Results from media-specific growth suggested the overgrown colonies were mostly Shigella and *E.coli* and it was proven by metagenomic data of cecal samples at the genus level (Fg.2(e) and 2(f)). An increase in Proteobacteria is concomitant with increased inflammation [54]. It is important to note that the Firmicutes (F) from 60-70% and Bacteroidetes (B) from 30-35% on day zero turned to 10% (F) and 1% or less (B) for both BALB/c and C57BL/6 on day 5 or day 4, respectively. This suggested increase in Firmicutes/Bacteroidetes (F/B) ratio is correlated with enhanced body mass index and inflammation [61]. Current results showed an increase in F/B ratio of 2-fold on day 0 to 10 fold or

more following treatment with vancomycin on day 5 for BALB/c or day 4 for C57BL/6. The F/B ratio significantly decreased after day 4 or 5 for C57BL/6 or BALB/c. It is further observed that the phylum, Verrucomicrobia level increased (20-25%) (63210 of total 316025 OTU) in BALB/c mouse (Fig. 1(d)) on the sixth day following treatment with vancomycin. Similarly, Verrucomicrobia increased significantly (>80%) (308845 of total 385907 OTU) from the fifth day following vancomycin treatment in C57BL/6 mice (Fig. 1(f)). We confirmed that the Akkermansia genus of Verrucomicrobia phylum increased from 2-3% (untreated group) to 70-75% by the fifth day following treatment with vancomycin in C57BL/6 mice (Fig. 2(d)). This result is significant to understand the differential response exhibited in two different mice species (C57BL/6 and BALB/c) used in this study following treatment with vancomycin. The differences observed maybe because of the immune bias (Th1 and Th2) of two species leading to different beneficial effects of Akkermansia to regulate glucose tolerance efficiency.

It is reported that *Akkermansia muciniphila* in the Verrucomicrobia phylum is the major known species that contributes positively to enhance insulin sensitivity and glucose metabolism by reducing inflammation and body-weight gain [62–64]. We, therefore, tested for *A. muciniphila* on day 6 following treatment with vancomycin of BALB/c and C57Bl/6. Species-specific primer (Table 2) of *Akkermansia muciniphila* was used to confirm its abundance [65]. Results revealed that there was a 6-fold increase in *A. muciniphila* abundance in vancomycin treated BALB/c on day 6 compared to time-matched untreated control while the abundance of *A. muciniphila* was around 16384-fold and 24833-fold higher in vancomycin treated C57BL/6 on day 5 and day 6 compared to its time-matched control. The current study revealed a hitherto unknown fact that abundance of *A. muciniphila* increases significantly following treatment with Vancomycin. The increase of *A. muciniphila* may have beneficial roles in physiology.

The inflammatory response, in gut, changes during vancomycin treatment in terms of dosage and with time

Pro- and anti-inflammatory responses are two important classes to check out the outcome of various treatments. Current results revealed that the expression of pro-inflammatory cytokines (tnfα, il6, il1a, il17), in the gut at transcriptional level, increased till day 5 for BALB/c mice (Fig. 3(a)) and till day 4 for C57BL/6 mice (Fig. 3(b)) following treatment with vancomycin. Concentration of anti-inflammatory cytokines (tgfb, and il10) started increasing and pro-inflammatory cytokines started decreasing from day 6 onwards in BALB/c mice (Fig. 3(c)) and from day 5 onwards in C57BL/6 mice (Fig. 3(d)) following treatment with vancomycin. Concomitant to the increase in pro-inflammatory cytokines we observed an increase in expression of tlr4 at transcriptional level till day 4 and tlr2 till day 6 in both BALB/C and C57BL/6 mice following treatment with vancomycin (Fig. 3(e) and Fig. 3(f)).

Major changes happened in the expression of tnfα and il10 at the transcriptional level, as revealed from qRT-PCR data, on 3rd- and 6th-day following treatment with vancomycin in both Th1- and Th2-biased mice. Validation of qRT PCR results was done, at the protein level expression by ELISA (Fig. 4). ELISA results revealed that on the third day following vancomycin treatment, TNFα level was significantly more in both BALB/C (Fig. 4(a)) and C57BL/6 (Fig. 4(b)) mice with respect to day 3 time-matched untreated control group of mice. Similarly, IL10 cytokine level was more in BALB/c (Fig. 4(c)) and C57BL/6 (Fig.4(d)) on day 6 following treatment with vancomycin compared to the day 6 time-matched untreated control mice. While changes in TNFα expression correspond well for both mice strain between transcriptional and protein level validation, we noted that the transcriptional changes for IL10 in BALB/c does not corroborate with protein level validation but it is validated for C57BL/6. The reason for such mismatch needs to be

explored further. It is important to note that the time kinetics (day 6 post vancomycin treatment), observed for enhanced anti-inflammatory (il10) response in either of the mouse strains, matches with the rise of *A. muciniphila*. The results might indicate hitherto unknown finding that an increase in *A. muciniphila* may lead to a transition from pro-inflammatory to anti-inflammatory response irrespective of initial immune bias of the mice. The observed transition from pro- to anti-inflammatory responses may be a combined effect of decreased level of Proteobacteria and elevated abundance of Verrucomicrobia.

Gut permeability increased following vancomycin treatment:

Gut permeability gets affected as a direct consequence of altered gut microbiota. Alteration of abundance and diversity of gut microbiota is measured in terms of the cecal index of the host (a measure of normalized cecal mass over body mass). The cecal index was calculated and the ratio was significantly more in vancomycin treated C57BL/6 and BALB/c mice than their respective time-matched control groups (Fig. 5(a)). Cecum is known to be a better representation than the fecal sample for understanding intestinal microbiota profile [66] and cecum usually gets enlarged following treatment with antibiotic by accumulating fluid and solid matter [67]. The changes in the bacterial composition due to antibiotic treatment in cecum may have led to the accumulation of a significantly high volume of fluid in its lumen. The fluid volume following centrifugation of cecal sample was significantly more in vancomycin treated mice than respective time-matched control mice (Fig. 5(b)). In vancomycin treated mice, a larger cecum with more fluid accumulation was observed than control mice (Fig. 5(c)). For further confirmation of gut permeability, FITC conjugated dextran was gavaged on day 3 following treatment with vancomycin and in respective control mice. FITC dextran Concentration was detected significantly higher in the serum of mice on day 3 following vancomycin treatment (BALB/c 341.6±25.9 ng/ml, C57BL/6 367.5±25.3

ng/ml) than corresponding time-matched control mice (BALB/c 217.1±24 ng/ml, C57BL/6 229.8±22 ng/ml). (Fig. 5(d)). The preceding observations on fluid accumulation and FITC-dextran results on gut permeability prompted us to check for respective gene expression. The results from qRT-PCR revealed compromised expression of tight junction genes (occludin and claudin) at the transcriptional level in the gut of vancomycin treated mice at different time points with respect to the time-matched control mice. Their expression of claudin gene decreased continuously from day one to day six following treatment with vancomycin in BALB/c (from 1.2-fold activation following vancomycin treatment with respect to time-matched control on day zero to 3.4-fold repression on day 6 by treatment with vancomycin when compared to time-matched untreated control) and C57BL/6 (From two-fold activation on day zero to 1.5-fold repression on day six when vancomycin treated mice re compared to untreated time-matched controls) mice (Fig. 5(e) and Fig. 5(f)). Similarly, expression of occludin gene decreased in BALB/c mice (from 2.5-fold activation on day zero to 6.5-fold repression on day six) and C57BL/6 (from 2.3- fold activation on day one to no-change on day six) following vancomycin treatment. It is important to note that the expression of claudin 1in C57BL/6 and occludin in both C57BL/6 and BALB/c mice, that were activated on day 1 following vancomycin treatment but significantly repressed following treatment with vancomycin on subsequent days. The results presented in Figs. 5(e) and 5(f), perhaps suggested that effects of vancomycin on the expression of gut permeable genes are very rapid. The results of gene expression corroborated with the FITC-dextran data to confirm reduced gut permeability following vancomycin treatment in both C57BL/6- and BALB/c mice. While results from FITC dextran studies on day 6 suggested restoration of the gut barrier for both BALB/c and C57BL/6 expression of claudin 1 and occludin genes remained repressed with respect to time-matched control mice. Further studies are required to understand this apparent discrepancy which

may be due to a different mechanism, independent of these two genes, that may exist to re-establish the gut barrier function.

The reduced gut permeability following treatment with vancomycin may lead to an increased level of systemic endotoxin level. The endotoxin level in serum correlates with increase in pathogenic gram-negative bacteria (proteobacteria) in the gut and compromised permeability and inflammation of gut tissue [68]. The endotoxin level was measured in the serum of control and vancomycin treated mice. On the third day of vancomycin treatment, endotoxin level was the highest in the serum of both BALB/c (0.82±0.07 EU/ml) and C57BL/6 (0.67±0.12 EU/ml) mice but on the sixth day, its level decreased (0.44±0.07 EU/ml in BALB/c and 0.16±0.05 EU/ml in C57BL/6 mice) and became similar with the control group of mice (Fig. 5(g)). The results may be corroborating with either enhanced level of beneficial bacteria on day 6 following vancomycin treatment as described below or due to decreased level of proteobacteria or both.

Alteration of blood glucose level with changes in Proteobacteria and Verrucomicrobia level in gut:

Glucose is an important metabolite to keep the energy requirement and balance in the body. It is also easy to measure in the host blood to determine the glucose metabolism status. Kinetics of oral glucose tolerance test (OGTT) from 0 to 90 minutes was done following 12h fasting of either strain of mice. From the glucose tolerance test, it was revealed that glucose metabolism was different in control and vancomycin treated mice (Fig. 6(a) and 6(b)). Important to note that the results from OGTT studies for control animals for both BALB/c and C57BL/6 remain unchanged on days 0, 3 and 6. On the day 3 following vancomycin treatment, fasting serum glucose levels in the Th2- and Th1-biased mice (BALB/c 194.6± 6.3 mg/dl and C57BL/6 186±6 mg/dl) were significantly higher than their time-matched control (BALB/c 115±3 mg/dl and C57BL/6 126±4 mg/dl). On day 6

following vancomycin treatment glucose levels in BALB/c was 148.6±7 mg/dl and in C57BL/6 was 103±5 mg/dl. On the sixth day of vancomycin treatment, BALB/c mice (VB6) had similar fasting glucose level in blood like control (CB) and C57BL/6 mice (VC6) had lower fasting glucose level than control (CC) mice. At fifteen-minute post glucose gavage, the elevation of glucose level in the blood of treated mice of the third day (VB3 295±14 mg/dl and VC3 333±8 mg/dl) was significantly higher than control (CB 215±12 mg/dl, CC 216±7 mg/dl) and sixth day post-vancomycin (VB6 235±5 mg/dl, VC6 200±9 mg/dl) mice (Figs. 6(a) and 6(b)). The metabolism rate of glucose in the blood of the sixth day vancomycin treated mice (VB6, VC6) was faster than the third day treated mice (VB3 and VC3). This rate was higher for VC6 than VB6. In VC6 group of mice, the glucose level in the blood came to normal rapidly and its concentration at ninety-minute post glucose gavage was similar with the control group in BALB/C mice and lower than the control group in C57BL/6 mice. In VB3 and VC3 group of mice, the glucose concentration in blood at ninety minutes was still higher than control.

Day 3 vancomycin treated mice were transplanted with cecal microbiota (CMT) of day 6 vancomycin treated mice (more abundant with *A. muciniphila*) to observe its efficacy on glucose metabolism. In CMT treated group of day 3 (following vancomycin treatment) mice, glucose level in serum decreases drastically in C57BL/6 mice (Fig. 6(b)) and became equivalent to control groups of mice but in BALB/c mice the effect was insignificant (Fig. 6(a)).

Metabolite level in serum changes following vancomycin treatment

It is believed that the short chain fatty acids (SCFA) are the microbes associated molecular patterns that could regulate the innate immunity of the host. The current results revealed that the ratio of abundance of acetate/lysine (Fig. 6(c)), butyrate/lysine (Fig. 6(d)) and propionate /threonine (Fig. 6(e)) in serum are reduced significantly on day 6 following treatment with vancomycin. The results

depicted in Figs. 6(c)-6(e) might indicate that conversion of SCFAs such as acetate and butyrate from lysine and propionate from threonine were perhaps significantly decreased in the gut of vancomycin-treated mice. The results revealed that the concentrations of acetate, butyrate, and propionate (Table 3) in the blood of vancomycin treated mice on day 6 were lower but their respective substrate concentrations (lysine, and threonine) were higher than control on day 6 post vancomycin treatment. Important to note here that concomitant with the Th1-(C57BL/6) and Th2-(BALB/c) bias of the mice one should expect lower level of abundance of SCFAs in control (untreated) C57Bl/6 (CC) and control BALB/c (CB) on day 0 and our results supported such proposition (Table 3). The results, however, further suggested accumulation of the substrate in blood and less detection of SCFA in the vancomycin treated day 6 group of mice (VB and VC on D6). Among vancomycin treated groups, BALB/c (VB) mice had lower SCFA production rate than C57BL/6 (VC) mice. We further validated the abundance of acetate in the serum of both BALB/c and C57BL/6 mice by using acetate detection kit (EOAC-100, San Francisco, USA). The results validated the abundance of acetate following vancomycin treatment in VB6 (Vancomycin treated BALB/c on day 6) and VC6 (Vancomycin treated C57BL/6 on day 6). The concentrations of acetate in VB6 was 23.9±1.4 μM while the concentration in CB6 (time matched untreated control of BALB/c) was 35.3±1.6 μM. The same in VC6 (Vancomycin treated C57BL/6 on day 6) was 22.2±4 μM while the concentration of acetate in respective time-matched untreated (control) group CC6 was 41.3±1.02 μM (Fig. 6(f)). The results implied for the first time the role of vancomycin on SCFA production in Th1- and Th2-biased mice. Results also supported the intrinsic SCFA production (more in Th2- compared to Th1-biased mice) as per the immune bias of mice strain.

Gut hormonal level during vancomycin treatment

We already reported that the rate of glucose metabolism increased and production of SCFAs decreased in the host on day 6 following the treatment with vancomycin. Considering the changes in glucose and SCFAs, we investigated further the roles of other associated hormones such as insulin and Peptide tyrosine tyrosine (PYY) in serum and also a control hormone leptin which is mostly activated in adipocytes [69–71]. Results (Fig. 7(a)) revealed that the concentration of insulin in serum on the third day of vancomycin treated a) BALB/c (VB3) was 1.16±0.25 ng/ml and b) C57BL/6 (VC3) was 1.43±0.15 ng/ml. Similarly, the concentration of insulin in serum on the sixth day of vancomycin treated a) BALB/c (VB6) was 0.98±0.1 ng/ml and b) C57BL/6 (VC6) was 0.83±0.06 ng/ml. Fig. 7(a) revealed that insulin level decreased significantly on day 6 compared to day 3 following treatment with vancomycin for both BALB/c and C57BL/6. However, insulin levels for both mice strains on day 3 and day 6 post-vancomycin were significantly higher than day 0 (untreated controls CB and CC). As hypothesized, no significant changes were observed in serum leptin concentrations on any day following vancomycin treatment of BALB/c and C57BL/6 mice with respect to respective untreated controls (Fig. 7(b)). The results revealed that the concentration of PYY hormone in the gut decreased following vancomycin treatment in BALB/c (8836±311 pg/mg of tissue on day 0 and 4843.9±149 on day 6) and in C57BL/6 mice (7883±155 pg/mg of tissue on day 0 to 6283.8±209 on day 6) (Fig.7(c)). As documented recently that SCFA regulates PYY production is validated by the current results [62]. Vancomycin treatment reduces SCFA level following a deceased abundance of PYY.

Discussion

It is reported that the treatment with Vancomycin reduces the abundance and diversity of the gut microbiota [29, 72]. The current study corroborated with the fact that mice treated with vancomycin had decreased levels of Firmicutes and Bacteroidetes and elevated levels of

Proteobacteria [29, 72]. The current report revealed via metagenomic (16S rRNA) analysis and plating data of cecal samples on specific media showed a significant increase in Shigella and *E.coli* bacteria of proteobacteria phylum in gut following the 4th day of treatment with vancomycin. It is apparent that the increase in the one phylum would repress the abundance of other phyla and as a sequela, the overall diversity of the gut microbiota would decrease [73]. In the current study, we observed an increase in the Proteobacteria decreases the diversity of the gut microbiota. Diversity was the lowest on days 4 and 5 following treatment with vancomycin for C57BL/6 and BALB/c mice, respectively. Escherichia and Shigella genera belong to gram-negative group of bacteria containing LPS, hence the endotoxin level in the blood increased [73, 74]. These bacteria activate the tlr4 receptor present in the gut epithelial cell, and this causes increases in the expression of pro-inflammatory cytokines [75]. In the current study, concerted effects of the increase in Proteobacteria and decrease in Firmicutes in mice gut caused increased inflammation in the gut tissue. Firmicutes, specifically Clostridium group present in the gut produces short-chain fatty acid like acetate, butyrate, propionate from complex carbohydrate foods [76]. Instentimonas bacteria (Firmicutes phylum) produces butyrate from lysine and Bacteroidetes produces propionate from threonine in the gut [73, 74]. The production of these SCFA in the gut suppresses the LPS and pro-inflammatory cytokines like TNF-α, IL-6 level and enhances the release of the anti-inflammatory cytokine like IL10 [36, 75]. The current study following treatment with Vancomycin established the decrease in Firmicutes and Bacteroidetes level significantly in mice gut. The decrease in these two phyla resulted less production of SCFA and subsequently prompted an increased level of inflammation in vancomycin treated mice compared to control mice.

It is well established that overexpression of Inflammatory cytokine like TNFα is associated with the higher gut permeability by suppressing the expression of tight junction proteins like occludin

and claudin 1 [77, 78]. Lower expression of tight junction protein in vancomycin treated mice caused the increase in gut permeability resulting in the higher cecal index and fluid accumulation of cecal sample. It is reported that increased abundance of Verrucomicrobia causes a decrease in inflammation and enhances glucose metabolism of the host [77–79]. On the sixth day of vancomycin treatment, the current results revealed a decrease in Proteobacteria and increase in Verrucomicrobia which might have caused an anti-inflammatory effect in the gut. During obesity and diabetic condition, metabolic endotoxemia had been observed where endotoxin (LPS) level increased in the blood to cause inflammation and impaired glucose metabolism in the host [80, 81]. The current reports revealed that the increase in Proteobacteria phylum in gut during vancomycin treatment elevated (highest effect was observed on day 3 following treatment) the endotoxin level of blood in mice to lead to impaired glucose metabolism and insulin resistance. On the sixth day, however, following vancomycin treatment, replacement of Proteobaceria by Verrucomicrobia caused significant improvement in glucose metabolism in mice by bringing back the fasting glucose and insulin level in blood to normalcy. This effect (reverting the blood glucose and insulin level to normal level) was more prevalent in C57BL/6 than BALB/c mice. Following successful transfer of the cecal sample from sixth day of vancomycin treated C57BL/6 mice (*A. muciniphila* level is above 70%) to the third day of vancomycin treated mice, blood glucose level, of day 3 mice, decreased significantly. Since day 6 mice had a significantly higher level of Akkermansia, the current report warrants more studies (ongoing in the current laboratory) to establish the effective causal role of *Akkermansia muciniphila* in controlling the blood glucose level. Higher concentration, of fasting Insulin and glucose in serum of BALB/c and C57BL/6 on day 3 following vancomycin treatment, than control and sixth day vancomycin treated mice established insulin resistance on day 3 following vancomycin treatment. Increase in the abundance

of *A. muciniphila* level in mice gut (especially in C57Bl/6) could have reversed the effects to bring back the glucose to a normal level as in control. On the sixth day of vancomycin treatment, *A. muciniphila* level was significantly higher in C57BL/6 mice than BALB/c, which might have caused more prominent effect in decreasing glucose level and increasing insulin sensitivity in the blood of C57BL/6 than BALB/c mice.

More SCFA usually leads to anti-inflammatory response or Th2-bias and our current observation further confirms the fact as per the immune bias of mice strain used. SCFA stimulated PYY hormone production by activating Gq coupled receptor FFA2 of endocrine cells present in the gut [62]. The current results revealed that following treatment with vancomycin the level of SCFA decreased, which cause a reduction in serum PYY production that might have an effect of observed enhanced glucose metabolism or increased insulin sensitivity [82]. We observed a decrease in insulin level in serum on day 6 than day 3 following treatment with vancomycin but blood glucose level was better managed on day 6 compared to day 3 perhaps suggesting enhanced insulin sensitivity.

The dose dependent perturbation of gut microbiota by vancomycin affects the host in two different ways; Initial doses caused increased in pathogenic bacteria in the gut which caused mostly deleterious effect on the host while continued later doses of vancomycin caused in increased verrucomicrobia phylum in the gut which showed some beneficial effects on the host.

Author Contribution Statement

PR performed all experiments drafted the manuscript. PR and PA designed the experiments. PA supervised the studies in general and also finalized the manuscript.

Funding & payment:

The current work was not supported through any extra-mural funding except the PhD fellowship to PR by the Council of Scientific and Industrial Research (CSIR), Govt. of India, India. Necessary resources to perform the experiment and the infra-structure for the laboratory were supported by the parent institute NISER. The current authors have no support to pay for the open-access or article processing fees to publish this research article.

Acknowledgment

This research received no specific grant from any funding agency in the public, commercial, or not-for-profit sectors. Authors extend their thanks to the NMR facility of NISER for assisting in collecting 1D proton-NMR FIDs and also thank the animal facility of NISER for their assistance. This manuscript has been released as a pre-print at BioRxiv (https://www.biorxiv.org/content/10.1101/516898v2).

Conflict of Interest

Authors declare that there is no conflict of interest.

References

1. **Jandhyala SM, Talukdar R, Subramanyam C, Vuyyuru H, Sasikala M, *et al.*** Role of the normal gut microbiota. *World J Gastroenterol WJG* 2015;21:8787.
2. **Andoh A**. Physiological role of gut microbiota for maintaining human health. *Digestion* 2016;93:176–181.
3. **Young VB**. The intestinal microbiota in health and disease. *Curr Opin Gastroenterol* 2012;28:63.
4. **Willing BP, Russell SL, Finlay BB**. Shifting the balance: Antibiotic effects on host-

microbiota mutualism. *Nature Reviews Microbiology* 2011;9:233–243.

5. **Guinane CM, Cotter PD**. Role of the gut microbiota in health and chronic gastrointestinal disease: understanding a hidden metabolic organ. *Therap Adv Gastroenterol* 2013;6:295–308.

6. **Thursby E, Juge N**. Introduction to the human gut microbiota. *Biochem J* 2017;474:1823–1836.

7. **Shanahan F**. The host–microbe interface within the gut. *Best Pract Res Clin Gastroenterol* 2002;16:915–931.

8. **O'Hara AM, Shanahan F**. The gut flora as a forgotten organ. *EMBO Rep* 2006;7:688–693.

9. **Dalby MJ, Ross AW, Walker AW, Morgan PJ**. Dietary uncoupling of gut microbiota and energy harvesting from obesity and glucose tolerance in mice. *Cell Rep* 2017;21:1521–1533.

10. **Wu H-J, Wu E**. The role of gut microbiota in immune homeostasis and autoimmunity. *Gut Microbes* 2012;3:4–14.

11. **Cani PD, Delzenne NM**. The role of the gut microbiota in energy metabolism and metabolic disease. *Curr Pharm Des* 2009;15:1546–1558.

12. **Ubeda C, Djukovic A, Isaac S**. Roles of the intestinal microbiota in pathogen protection. *Clin Transl Immunol*;6.

13. **Palmer C, Bik EM, DiGiulio DB, Relman DA, Brown PO**. Development of the human infant intestinal microbiota. *PLoS Biol* 2007;5:e177.

14. **Hill CJ, Lynch DB, Murphy K, Ulaszewska M, Jeffery IB, *et al.*** Evolution of gut microbiota composition from birth to 24 weeks in the INFANTMET Cohort. *Microbiome*

2017;5:4.

15. **Singh RK, Chang H-W, Yan D, Lee KM, Ucmak D, *et al.*** Influence of diet on the gut microbiome and implications for human health. *J Transl Med* 2017;15:73.

16. **Falony G, Joossens M, Vieira-Silva S, Wang J, Darzi Y, *et al.*** Population-level analysis of gut microbiome variation. *Science (80-)* 2016;352:560–564.

17. **Morton ER, Lynch J, Froment A, Lafosse S, Heyer E, *et al.*** Variation in rural African gut microbiota is strongly correlated with colonization by Entamoeba and subsistence. *PLoS Genet* 2015;11:e1005658.

18. **Bendtsen KMB, Krych L, Sørensen DB, Pang W, Nielsen DS, *et al.*** Gut microbiota composition is correlated to grid floor induced stress and behavior in the BALB/c mouse. *PLoS One* 2012;7:e46231.

19. **Khan CM**. The dynamic interactions between Salmonella and the microbiota, within the challenging niche of the gastrointestinal tract. *Int Sch Res Not*;2014.

20. **Lange K, Buerger M, Stallmach A, Bruns T**. Effects of antibiotics on gut microbiota. *Dig Dis* 2016;34:260–268.

21. **Jernberg C, Löfmark S, Edlund C, Jansson JK**. Long-term impacts of antibiotic exposure on the human intestinal microbiota. *Microbiology* 2010;156:3216–3223.

22. **Fujisaka S, Ussar S, Clish C, Devkota S, Dreyfuss JM, *et al.*** Antibiotic effects on gut microbiota and metabolism are host dependent. *J Clin Invest* 2016;126:4430–4443.

23. **Dethlefsen L, Huse S, Sogin ML, Relman DA**. The pervasive effects of an antibiotic on the human gut microbiota, as revealed by deep 16S rRNA sequencing. *PLoS Biol* 2008;6:e280.

24. **Dunlop SP, Hebden J, Campbell E, Naesdal J, Olbe L, *et al.*** Abnormal intestinal

permeability in subgroups of diarrhea-predominant irritable bowel syndromes. *Am J Gastroenterol* 2006;101:1288.

25. **Bosi E, Molteni L, Radaelli MG, Folini L, Fermo I, *et al.*** Increased intestinal permeability precedes clinical onset of type 1 diabetes. *Diabetologia* 2006;49:2824–2827.

26. **Pepin J**. Vancomycin for the treatment of Clostridium difficile infection: for whom is this expensive bullet really magic? *Clin Infect Dis* 2008;46:1493–1498.

27. **Tang J, Hu J, Kang L, Deng Z, Wu J, *et al.*** The use of vancomycin in the treatment of adult patients with methicillin-resistant Staphylococcus aureus (MRSA) infection: a survey in a tertiary hospital in China. *Int J Clin Exp Med* 2015;8:19436.

28. **Bernard L, Vaudaux P, Vuagnat A, Stern R, Rohner P, *et al.*** Effect of vancomycin therapy for osteomyelitis on colonization by methicillin-resistant Staphylococcus aureus: lack of emergence of glycopeptide resistance. *Infect Control Hosp Epidemiol* 2003;24:650–654.

29. **Isaac S, Scher JU, Djukovic A, Jiménez N, Littman DR, *et al.*** Short-and long-term effects of oral vancomycin on the human intestinal microbiota. *J Antimicrob Chemother* 2016;72:128–136.

30. **Reijnders D, Goossens GH, Hermes GDA, Neis EPJG, van der Beek CM, *et al.*** Effects of Gut Microbiota Manipulation by Antibiotics on Host Metabolism in Obese Humans: A Randomized Double-Blind Placebo-Controlled Trial. *Cell Metab*. Epub ahead of print 2016. DOI: 10.1016/j.cmet.2016.06.016.

31. **Watanabe H, Numata K, Ito T, Takagi K, Matsukawa A**. Innate immune response in Th1- and Th2-dominant mouse strains. *Shock*. Epub ahead of print 2004. DOI: 10.1097/01.shk.0000142249.08135.e9.

32. **Jovicic N, Jeftic I, Jovanovic I, Radosavljevic G, Arsenijevic N, *et al.*** Differential immunometabolic phenotype in Th1 and Th2 dominant mouse strains in response to high-fat feeding. *PLoS One*. Epub ahead of print 2015. DOI: 10.1371/journal.pone.0134089.

33. **Hooper L V, Littman DR, Macpherson AJ**. Interactions between the microbiota and the immune system. *Science (80-)* 2012;336:1268–1273.

34. **Watanabe H, Numata K, Ito T, Takagi K, Matsukawa A**. Innate immune response in Th1- and Th2-dominant mouse strains. *Shock* 2004;22:460–6.

35. **Christiansen CB, Gabe MBN, Svendsen B, Dragsted LO, Rosenkilde MM, *et al.*** The impact of short chain fatty acids on GLP-1 and PYY secretion from the isolated perfused rat colon. *Am J Physiol Liver Physiol*.

36. **Morrison DJ, Preston T**. Formation of short chain fatty acids by the gut microbiota and their impact on human metabolism. *Gut Microbes* 2016;7:189–200.

37. **Turner JR**. Intestinal mucosal barrier function in health and disease. *Nat Rev Immunol* 2009;9:799.

38. **Ulluwishewa D, Anderson RC, McNabb WC, Moughan PJ, Wells JM, *et al.*** Regulation of tight junction permeability by intestinal bacteria and dietary components. *J Nutr* 2011;141:769–776.

39. **Erikstrup LT, Aarup M, Hagemann-Madsen R, Dagnaes-Hansen F, Kristensen B, *et al.*** Treatment of Clostridium difficile infection in mice with vancomycin alone is as effective as treatment with vancomycin and metronidazole in combination. *BMJ open Gastroenterol* 2015;2:e000038.

40. **Patel S, Preuss C V., Bernice F**. *Vancomycin*. StatPearls Publishing; 2019.

41. **Pradhan B, Guha D, Naik AK, Banerjee A, Tambat S, *et al.*** Probiotics L. acidophilus

and B. clausii Modulate Gut Microbiota in Th1- and Th2-Biased Mice to Ameliorate Salmonella Typhimurium-Induced Diarrhea. *Probiotics Antimicrob Proteins*. Epub ahead of print 16 June 2018. DOI: 10.1007/s12602-018-9436-5.

42. **Ghosh A, Mukherjee R, Aich P, Naik AK, Chakraborty S, *et al.*** Lactobacillus rhamnosus GG reverses mortality of neonatal mice against Salmonella challenge. *Toxicol Res (Camb)*. Epub ahead of print 2019. DOI: 10.1039/c9tx00006b.

43. **Dekker JP, Frank KM**. Salmonella, Shigella, and Yersinia. *Clinics in Laboratory Medicine* 2015;35:225–246.

44. **Guha D, Banerjee A, Mukherjee R, Pradhan B, Peneva M, *et al.*** A probiotic formulation containing Lactobacillus bulgaricus DWT1 inhibits tumor growth by activating pro-inflammatory responses in macrophages. *J Funct Foods* 2019;56:232–245.

45. **Pradhan B, Guha D, Ray P, Das D, Aich P**. Comparative Analysis of the Effects of Two Probiotic Bacterial Strains on Metabolism and Innate Immunity in the RAW 264.7 Murine Macrophage Cell Line. *Probiotics Antimicrob Proteins*. Epub ahead of print 2016. DOI: 10.1007/s12602-016-9211-4.

46. **Kim JJ, Shajib MS, Manocha MM, Khan WI**. Investigating intestinal inflammation in DSS-induced model of IBD. *J Vis Exp JoVE*.

47. **Mysara M, Njima M, Leys N, Raes J, Monsieurs P**. From reads to operational taxonomic units: an ensemble processing pipeline for MiSeq amplicon sequencing data. *Gigascience* 2017;6:1–10.

48. **Purcell R V, Visnovska M, Biggs PJ, Schmeier S, Frizelle FA**. Distinct gut microbiome patterns associate with consensus molecular subtypes of colorectal cancer. *Sci Rep* 2017;7:11590.

49. **Caporaso JG, Kuczynski J, Stombaugh J, Bittinger K, Bushman FD, *et al.*** QIIME allows analysis of high-throughput community sequencing data. *Nat Methods* 2010;7:335.

50. **Kastenberger I, Lutsch C, Herzog H, Schwarzer C**. Influence of sex and genetic background on anxiety-related and stress-induced behaviour of prodynorphin-deficient mice. *PLoS One* 2012;7:e34251.

51. **DeSantis TZ, Hugenholtz P, Larsen N, Rojas M, Brodie EL, *et al.*** Greengenes, a chimera-checked 16S rRNA gene database and workbench compatible with ARB. *Appl Environ Microbiol* 2006;72:5069–5072.

52. **DeSantis TZ, Hugenholtz P, Keller K, Brodie EL, Larsen N, *et al.*** NAST: A multiple sequence alignment server for comparative analysis of 16S rRNA genes. *Nucleic Acids Res* 2006;34:394–399.

53. **Frank DN, Amand ALS, Feldman RA, Boedeker EC, Harpaz N, *et al.*** Molecular-phylogenetic characterization of microbial community imbalances in human inflammatory bowel diseases. *Proc Natl Acad Sci* 2007;104:13780–13785.

54. **Zhou Y, Zhi F**. Lower level of bacteroides in the gut microbiota is associated with inflammatory bowel disease: a meta-analysis. *Biomed Res Int*;2016.

55. **Xia J, Wishart DS**. Web-based inference of biological patterns, functions and pathways from metabolomic data using MetaboAnalyst. *Nat Protoc* 2011;6:743.

56. **Xia J, Sinelnikov I V, Han B, Wishart DS**. MetaboAnalyst 3.0—making metabolomics more meaningful. *Nucleic Acids Res* 2015;43:W251–W257.

57. **Hapfelmeier S, Stecher B, Barthel M, Kremer M, Müller AJ, *et al.*** The Salmonella pathogenicity island (SPI)-2 and SPI-1 type III secretion systems allow Salmonella serovar typhimurium to trigger colitis via MyD88-dependent and MyD88-independent

mechanisms. *J Immunol* 2005;174:1675–1685.

58. **Vazquez-Torres A, Vallance BA, Bergman MA, Finlay BB, Cookson BT, *et al.*** Toll-like receptor 4 dependence of innate and adaptive immunity to Salmonella: importance of the Kupffer cell network. *J Immunol* 2004;172:6202–6208.

59. **Woting A, Blaut M**. Small Intestinal Permeability and Gut-Transit Time Determined with Low and High Molecular Weight Fluorescein Isothiocyanate-Dextrans in C3H Mice. *Nutrients* 2018;10:685.

60. **Holzheimer RG**. Antibiotic Induced Endotoxin Release and Clinical Sepsis: a Review. *J Chemother* 2001;13:159–172.

61. **Koliada A, Syzenko G, Moseiko V, Budovska L, Puchkov K, *et al.*** Association between body mass index and Firmicutes/Bacteroidetes ratio in an adult Ukrainian population. *BMC Microbiol* 2017;17:120.

62. **FUJISAKA S, USUI I, NAWAZ A, IGARASHI Y, KADO T, *et al.*** Bofutsushosan Improves Gut Barrier Function with a Bloom of Akkermansia Muciniphila and Improves Glucose Metabolism in Diet-Induced Obese Mice. *Diabetes* 2018;67:1990-P.

63. **Khan MT, Nieuwdorp M, Bä Ckhed F**. Cell Metabolism Perspective Microbial Modulation of Insulin Sensitivity. *Cell Metab* 2014;20:753–760.

64. **Cani PD, de Vos WM**. Next-Generation Beneficial Microbes: The Case of Akkermansia muciniphila. *Front Microbiol*;8. Epub ahead of print 22 September 2017. DOI: 10.3389/fmicb.2017.01765.

65. **Collado MC, Derrien M, Isolauri E, De Vos WM, Salminen S**. Intestinal integrity and Akkermansia muciniphila, a mucin-degrading member of the intestinal microbiota present in infants, adults, and the elderly. *Appl Environ Microbiol*. Epub ahead of print 2007.

DOI: 10.1128/AEM.01477-07.

66. **Donaldson GP, Lee SM, Mazmanian SK**. Gut biogeography of the bacterial microbiota. *Nat Rev Microbiol* 2016;14:20.

67. **Reikvam DH, Erofeev A, Sandvik A, Grcic V, Jahnsen FL, *et al.*** Depletion of murine intestinal microbiota: Effects on gut mucosa and epithelial gene expression. *PLoS One*. Epub ahead of print 2011. DOI: 10.1371/journal.pone.0017996.

68. **Holzheimer RG**. Antibiotic Induced Endotoxin Release and Clinical Sepsis: a Review. *J Chemother*. Epub ahead of print 2014. DOI: 10.1179/joc.2001.13.supplement-2.159.

69. **Larraufie P, Martin-Gallausiaux C, Lapaque N, Dore J, Gribble FM, *et al.*** SCFAs strongly stimulate PYY production in human enteroendocrine cells. *Sci Rep* 2018;8:74.

70. **Woods SC, D'Alessio DA**. Central control of body weight and appetite. *Journal of Clinical Endocrinology and Metabolism*. Epub ahead of print 2008. DOI: 10.1210/jc.2008-1630.

71. **Xiong Y, Miyamoto N, Shibata K, Valasek MA, Motoike T, *et al.*** Short-chain fatty acids stimulate leptin production in adipocytes through the G protein-coupled receptor GPR41. *Proc Natl Acad Sci*. Epub ahead of print 2004. DOI: 10.1073/pnas.2637002100.

72. **Sun L, Zhang X, Zhang Y, Zheng K, Xiang Q, *et al.*** Antibiotic-induced disruption of gut microbiota alters local metabolomes and immune responses. *Front Cell Infect Microbiol*;9. Epub ahead of print 2019. DOI: 10.3389/fcimb.2019.00099.

73. **Maldonado RF, Sa-Correia I, Valvano MA, Mosca A, Leclerc M, *et al.*** The intestinal microbiota in health and disease. 2012.

74. **Steimle A, Autenrieth IB, Frick JS**. Structure and function: Lipid A modifications in commensals and pathogens. *International Journal of Medical Microbiology*

2016;306:290–301.

75. **Rallabhandi P, Awomoyi A, Thomas KE, Phalipon A, Fujimoto Y, *et al.*** Differential Activation of Human TLR4 by Escherichia coli and Shigella flexneri 2a Lipopolysaccharide: Combined Effects of Lipid A Acylation State and TLR4 Polymorphisms on Signaling . *J Immunol* 2008;180:1139–1147.

76. **Mosca A, Leclerc M, Hugot JP**. Gut microbiota diversity and human diseases: Should we reintroduce key predators in our ecosystem? *Front Microbiol*;7. Epub ahead of print 31 March 2016. DOI: 10.3389/fmicb.2016.00455.

77. **Hakansson A, Molin G**. Gut microbiota and inflammation. *Nutrients* 2011;3:637–82.

78. **Fujio-Vejar S, Vasquez Y, Morales P, Magne F, Vera-Wolf P, *et al.*** The gut microbiota of healthy chilean subjects reveals a high abundance of the phylum verrucomicrobia. *Front Microbiol* 2017;8:1221.

79. **Plovier H, Everard A, Druart C, Depommier C, Van Hul M, *et al.*** A purified membrane protein from Akkermansia muciniphila or the pasteurized bacterium improves metabolism in obese and diabetic mice. *Nat Med* 2017;23:107.

80. **Hawkesworth S, Moore SE, Fulford AJC, Barclay GR, Darboe AA, *et al.*** Evidence for metabolic endotoxemia in obese and diabetic Gambian women. *Nutr Diabetes* 2013;3:e83.

81. **Boutagy NE, McMillan RP, Frisard MI, Hulver MW**. Metabolic endotoxemia with obesity: Is it real and is it relevant? *Biochimie* 2016;124:11–20.

82. **Cahill F, Ji Y, Wadden D, Amini P, Randell E, *et al.*** The association of serum total peptide YY (PYY) with obesity and body fat measures in the coding study. *PLoS One*. Epub ahead of print 2014. DOI: 10.1371/journal.pone.0095235.

Figure Legends

Fig 1.

Phylum level changes in the gut microbiota. Time-dependent changes in the phyla of gut microbiota, in the control (a). BALB/c and (c). C57BL/6 and in vancomycin treated (b). BALB/c and (d). C57BL/6 mice are shown. In the figure, only major phyla are shown to avoid clutter. Data shown are average of 3 biological replicates. To avoid clutter, standard deviation (SD) calculated using 2-way ANOVA is not shown. However, SD was less than 10% on average. Kinetics of changes in phylum-level Equitability index (E) (diversity) of the gut microbiota following treatment with vancomycin in (e) BALB/c and (f) C57/BL6 mice. Statistical significance of diversity in panels (e) and (f) are shown by the letters a, and b among the treatment conditions that are significantly ('a', and 'b' correspond to $P \leq 0.001$) different. Error bars are one standard deviation of the mean value and determined from the average values of three biological replicates.

Fig 2.

Metataxonomic studies of the genus-level variation of gut microbiota in vancomycin treated and its respective control group. Kinetics of changes in genera of gut microbiota, in the control (a) BALB/c, and (c) C57BL/6 and in vancomycin treated (b) BALB/c, and (d) C57BL/6 mice are shown. Data shown are average of 3 biological replicates and standard deviation was less than 10% on average. Percentage abundance of different genera for various treatment conditions are shown on the 'Y'-axis and the days elapsed post treatment or for time-matched control are shown on the 'X'-axis. Colony of culturable Proteobacteria by plating of cecal samples from both strains of mice on selective and differential media. Evidence of (e) Shigella colonies growth on Salmonella-Shigella specific media agar plate on day 4 (CC) control C57BL/6, (VC) vancomycin

treated C57BL/6, (CB) control BALB/c and (VB) vancomycin treated BALB/c and (f) Growth of *E. coli*. colonies on EMB (Eosin methylene blue agar plate) on day 4 (VC) vancomycin treated C57BL/6 and (CC) control C57BL/6.

Fig 3.

Transcriptional gene expression profile. Kinetics of transcriptional (by qRT-PCR) expression of genes categorized as, pro-inflammatory in (a) BALB/c, and (b) C57BL/6, anti-inflammatory in (c) BALB/c, and (d) C57BL/6 as Toll like receptors tlr4 and tlr2 in (e) BALB/c, and (f) C57BL/6 mice. Statistical significance was calculated by two-way ANOVA and changes are denoted by the letters a, b, and c among the genes that are significantly ('a', and 'b' correspond to $P \leq 0.001$ while 'c' corresponds to $P \leq 0.01$) different. Error bars are one standard deviation of the mean value and determined from the average values of three biological replicates.

Fig 4.

Protein level gene expression and comparative analysis of qRT PCR and ELISA data for TNFα and IL10. (a) Mean values (n=3) of protein level concentration (in pg/mg) with standard deviation of TNFα (blue) and IL10 (red) expression on days 0, 3 and 6 for control and vancomycin treated BALB/c (CB and VB) and C57BL/6 (CC and VC) are shown. Statistical significance was calculated by two-way ANOVA and changes are denoted by the letters a, b, and c among the genes that are significantly ('a', and 'b' correspond to $P \leq 0.001$ while 'c' corresponds to $P \leq 0.01$) different. The genes that are compared for significance have the same letter. Fold change values of expression of TNFα (blue) and IL10 (red) to compare the values obtained from qRT-PCR and ELISA studies are shown for (b) BALB/c, and (c) C57BL/6. Error bars of the data are already shown in preceding figures.

Fig 5.

Measurement of intestinal integrity of BALB/c and C57BL/6 mice following treatment with Vancomycin. Changes in (a) Cecal index (total cecal mass/total body mass), and (b) Cecal liquid content in control (untreated) and vancomycin treated BALB/c and C57BL/6 mice are shown as bar plot. (c) Representative images of various sizes of Cecum from both BALB/c and C57BL/6 mice on day 6 following vancomycin treatment for 1. C57BL/6, and 2. BALB/c and corresponding time matched (day 6) untreated control for 3. C57BL/6 and 4. BALB/c are shown. (d) Gut permeability data by measuring FITC dextran concentration in serum of BALB/c and C57BL/6 on day 0 (control) and on day 3 and day 6 following treatment with vancomycin. Transcriptional expression levels of tight junction genes, claudin 1 and occluding, in gut tissue by qRT-PCR are shown in vancomycin treated and untreated (control) groups for (e) BALB/c and (f) C57BL/6 mice. Endotoxin concentration in the serum for both strains of mice are shown in panel (g), where CB, VB3 and VB6 implies untreated (control) and day 3 (D3) and day 6 (D6) post vancomycin treated BALB/c and CC, VC3 and VC6 denote the same for C57Bl/6 mice. The colors corresponding to different days are shown above the panels (e) and (f) Comparisons among the groups were calculated by two-way ANOVA. In the figure for panels (a), (b), (d). and (g), '***' corresponds to $P \leq 0.001$, '**' corresponds to $P \leq 0.01$, '*' corresponds to $P \leq 0.05$ level of significance). In panels, (e) and (f), significance among groups are indicated by 'a' and 'b' to avoid clutter. Error bars shown are one standard deviation from the mean value of four replicates (n=4).

Fig 6.

Glucose tolerance and abundance of select metabolites in serum. Kinetics of fasting blood sugar in (a) BALB/c (b) C57BL/6 mice following treatment with Vancomycin on days 0, 3 and 6 and

following treatment with CMT from day 6 vancomycin treated mice transferred to vancomycin treated day 3 group of mice. Ratio of abundance, from chemometric $_1$H-NMR studies for major short-chain fatty acids, of (c) acetate production over lysine, (d) butyrate production over lysine and (e) propionate production over threonine in untreated control BALB/c (CB) and C57BL/6 (CC) and Vancomycin treated BALB/c (VB) and C57BL/6 (VC) are compared for Day 0 and Day 6 following treatment with vancomycin. In addition, (f) acetate concentration in the serum by using acetate detection kit on day 6 in vancomycin treated groups of mice (VB6, VC6) along with the time-matched control mice (CB6, CC6) of BALB/c and C57BL/6, respectively. In the figure, '***' corresponds to $P \leq 0.001$, '**' corresponds to $P \leq 0.01$, level of significance). For panels '(c)', '(d)' and '(e)', the significant difference is shown by letters 'a' and 'b' as applicable and both letters indicated $P \leq 0.001$. Error bars shown are one standard deviation from the mean value of four replicates (n=4).

Fig 7.

Changes in select hormones in serum. Abundance of (a) Insulin (ng/ml), (b) Leptin (ng/ml) and (c) PYY (pg/mg) in the serum of control BALB/c (CB) or C57BL/6 (CC) and vancomycin treated mice on third day (VB3, VC3) and sixth day (VB6, VC6) of BALB/c and C57BL/6 mice respectively. Comparisons among the groups were calculated with two-way ANOVA. In the figure, '***' corresponds to $P \leq 0.001$, '**' corresponds to $P \leq 0.01$, '*' corresponds to $P \leq 0.05$ level of significance). Error bars shown are one standard deviation from the mean value of four replicates (n=4).

Tables

Table 1. Diversity assessment of Phylum and Genus for BALB/c and C57BL/6 following treatment with vancomycin.

Days post treatment	**Phylum**		**Genus**	
	Evenness[a] (± SD)			
	BALB/c	**C57BL/6**	**BALB/c**	**C57BL/6**
0	0.4(±0.05)	0.4(±0.06)	0.7(±0.01)	0.8(±0.03)
2	0.4(±0.07)	0.3(±0.03)	0.5(±0.05)	0.6(±0.04)
3	0.3(±0.06)	0.3(±0.01)	0.7(±0.03)	0.6(±0.08)
4	0.2(±0.04)	0.3(±0.04)	0.5(±0.04)	0.7(±0.06)
5	0.1(±0.06)	0.3(±0.01)	0.6(±0.08)	0.8(±0.05)
6	0.7(±0.04)	0.5(±0.08)	0.6(±0.06)	0.3(±0.12)

[a] Evenness, calculated based on diversity from Shannon Index

Table 2: Sequences of forward (_F) and reverse (_R) primers for PCR studies to confirm presence and expression level of

various genes used in this study.

Genes specific for	Sequence of the primers used
***A. muciniphila*_F**	5’-CAGCACGTGAAGGTGGGGAC-3’
***A. muciniphila*_R**	5’- CCTTGCGGTTGGCTTCAGAT-3'
***il10*_F**	5’-AGGCAGTGGAGCAGGTGAAGAGTG-3’
***il10*_R**	5’-GCTCTCAAGTGTGGCCAGCCTTAG-3’
***tnf*_F**	5’-CCACGTCGTAGCAAACCACCAAAG-3’
***tnf*_R**	5’- TGCCCGGACTCCGCAAAGTCTAAG-3’
***cldn1*_F**	5’-TGCCCCAGTGGAAGATTTACT-3’
***cldn1*_R**	5’-CTTTGCGAAACGCAGGACAT-3’
***tlr4*_F**	5’- CGCTGCCACCAGTTACAGAT-3’
***tlr4*_R**	5’-AGGAACTACCTCTATGCAGGGAT-3’
***ocln*_F**	5'- GTTGAACTGTGGATTGGCAG -3'
***ocln*_R**	5'- AAGATAAGCGAACCTTGGCG -3'
***il6*_F**	5'-AGACAAAGCCAGAGTCCTTCAGAG-3’
***il6*-R**	5’-CCACAGTGAGGAATGTCCACAAAC-3’
***tlr2*-F**	5’-GCCCGTAGATGAAGTCAGCTCACC-3’
***tlr2*-R**	5’-CGGGCATCTACTTCAGTCGAGTGG-3’
***il17*_F**	5’-TCCAGAAGGCCCTCAGACTA-3’
il17_R	5’-ACACCCACCAGCATCTTCTCA-3’
***tgfb*_F**	5’-CCCAGCATCTGCAAAGCT-3’

***tgfb*_R**	5'-GTCAATGTACAGCTGCCGCA-3'
***il1a*_F**	5'-ATCAGTACCTCACGGCTGCT-3'
***il1a*_R**	5'-TGGGTATCTCAGGCATCTCC-3'

Table 3. Abundance of various SCFAs and associated metabolites in untreated (control) and vancomycin treated BALB/c and C57BL/6

Days post treatment	**Mouse**	**Treatment**	**Condition**	**Acetate**	**Butyrate**	**Lysine**	**Propionate**	**Threonine**
				Mean concentration [μM] (± SD)				
0	BALB/c	None (Control)	CB0	149(±9.5)	231.4(±11.4)	183.8(±7.8)	216.6(±2)	105.1(±6.9)
0	BALB/c	Vancomycin	VB0	136.2(±7.4)	242(±13.6)	187.1(±1.3)	221.5(±5.7)	102.5(±10)
6	BALB/c	None (Control)	CB6	157.5(±4.9)	223.2(±18.3)	179(±8.5)	223.2(±5.9)	115.7(±7.6)
6	BALB/c	Vancomycin	VB6	54.3(±5.7)	65.9(±17.1)	275.6(±9.1)	119.8(±10.6)	293.9(±7.1)
0	C57BL/6	None (Control)	CC0	93.2(±3)	147.7(±3.5)	197.3(±1.6)	144.1(±4.3)	265.4(±14.2)

0	C57BL/6	Vancomycin	VC0	90.4(±2.1)	135.3(±14.3)	189(±4.9)	145.6(±9.3)	240.7(±11.6)
6	C57BL/6	None (Control)	CC6	94.6(±3.5)	130.8(±6.3)	199.6(±2.6)	132.6(±3.7)	248(±19.8)
6	C57BL/6	Vancomycin	VC6	70(±0.6)	76.6(±12.2)	219.8(±7.8)	91.8(±12.6)	278.4(±8.7)

Results for day 0 and day 6 for control and treated mice are shown

Figures

Fig. 1.

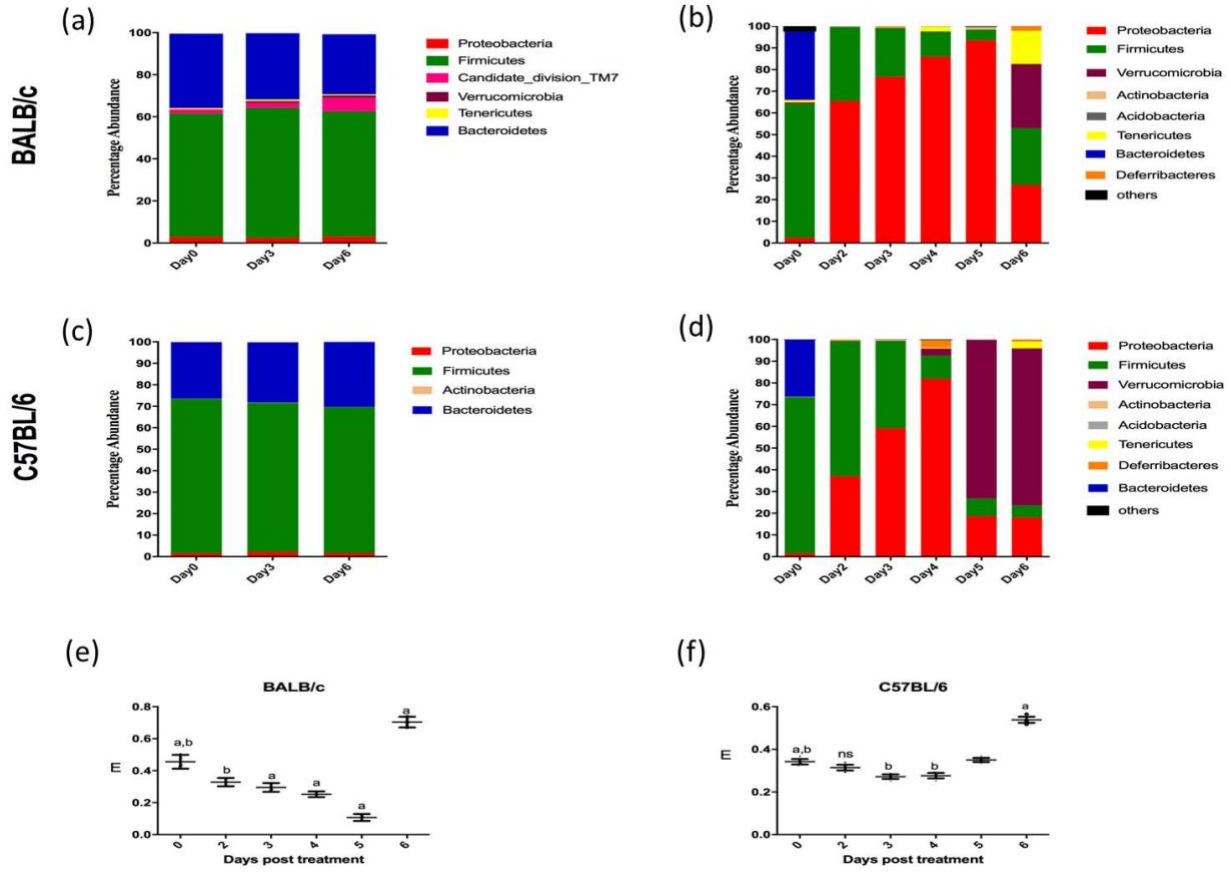

Fig. 2.

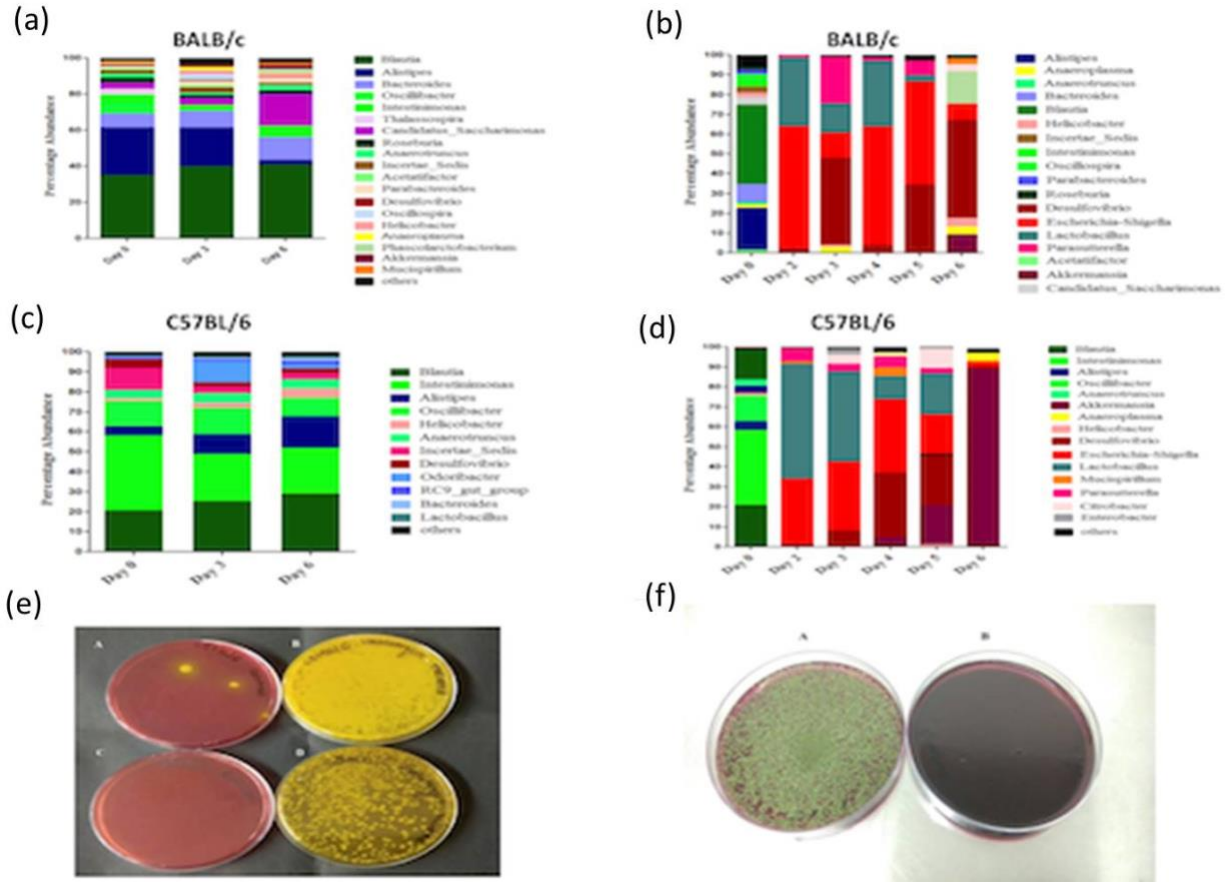

Fig. 3.

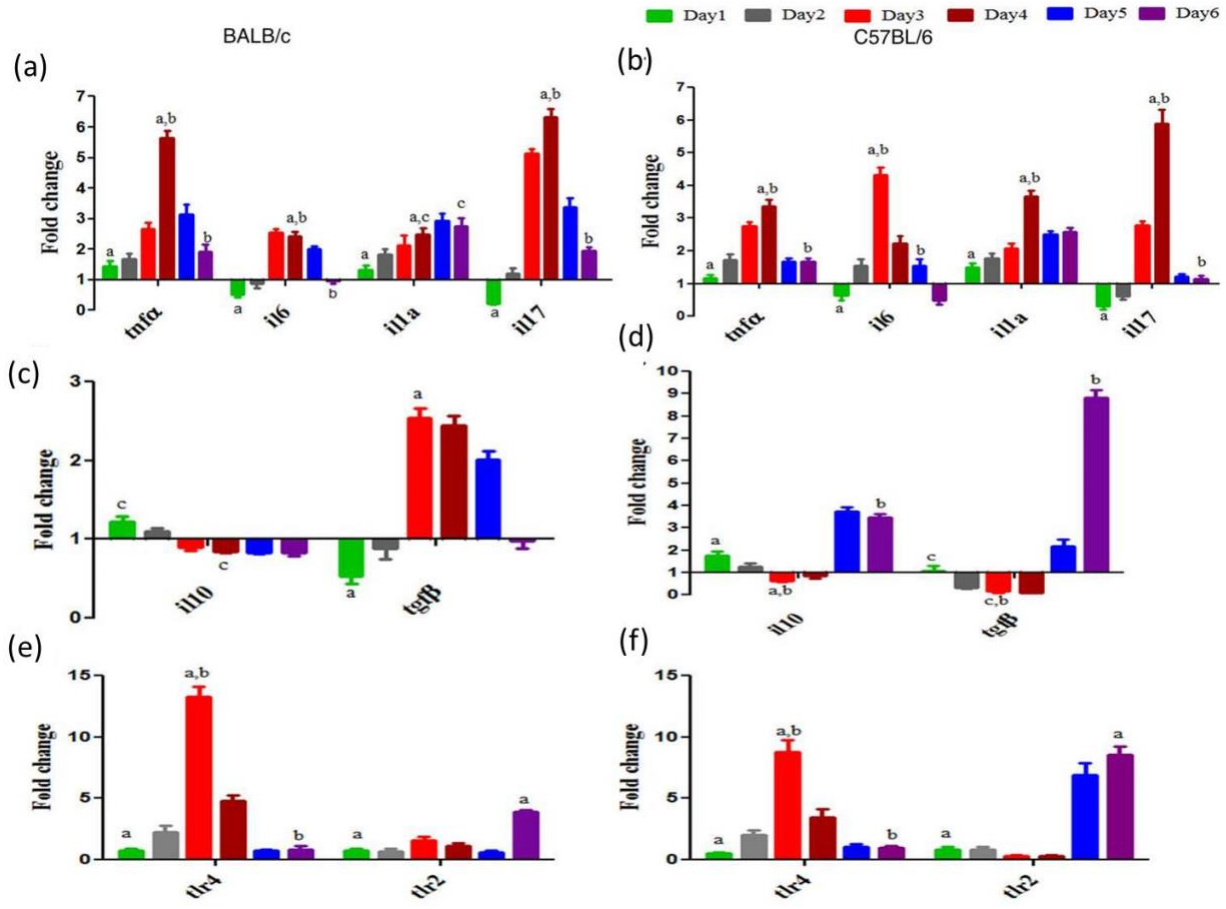
Day1
Day2
Day3
Day4
Day5
Day6
BALB/c
C57BL/6
(a)
(b)
(c)
(d)
(e)
(f)
Fold change
tnfα
il6
il1a
il17
il10
tgfβ
th4
th2

Fig. 4.

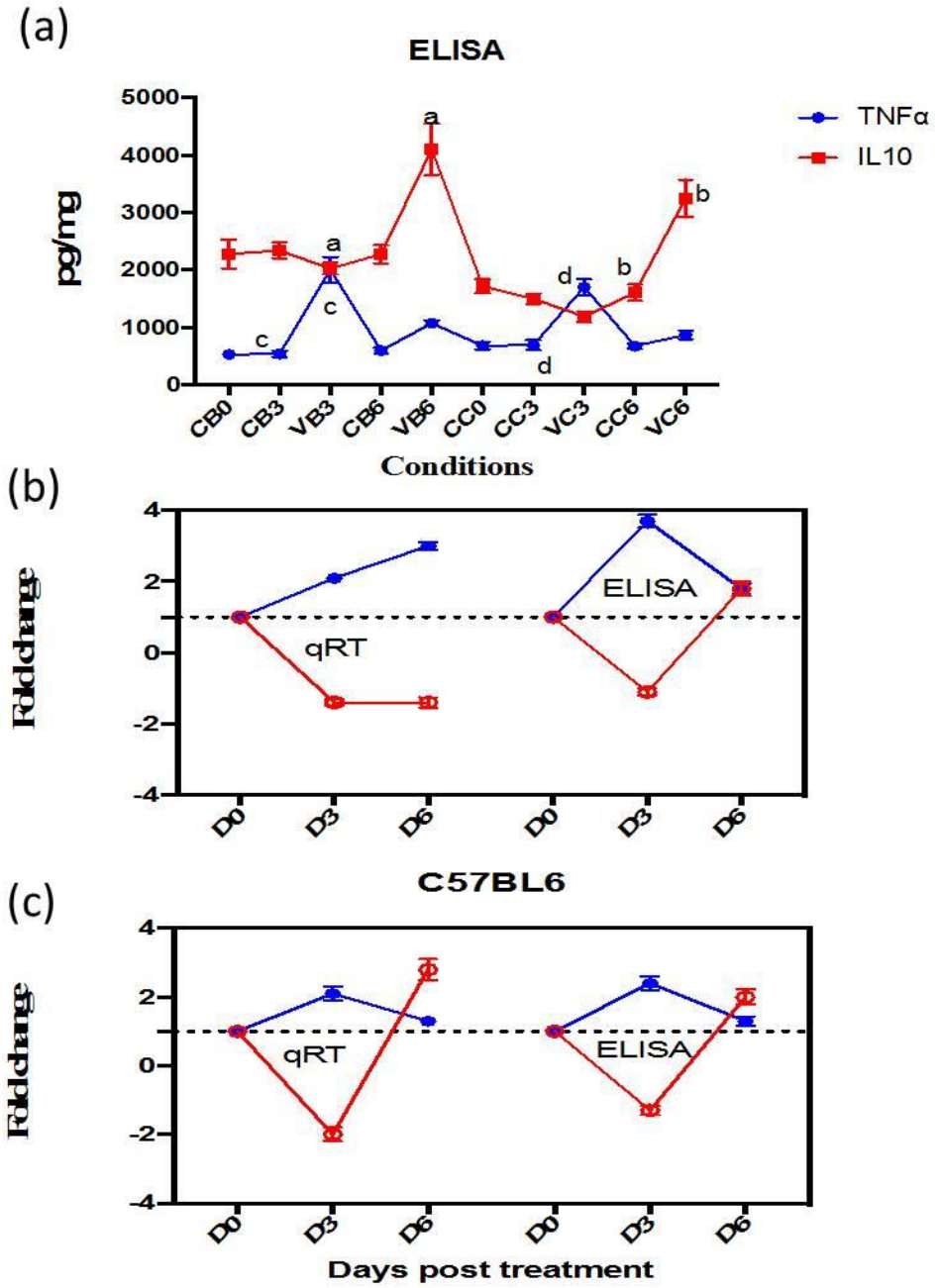
(a)
ELISA
pg/mg
5000
4000
3000
2000
1000
0
TNFα
IL10
a
b
c
d
CB0
CB3
VB3
CB6
VB6
CC0
CC3
VC3
CC6
VC6
Conditions
(b)
Fold change
4
2
0
-2
-4
ELISA
qRT
D0
D3
D6
(c)
C57BL6
Fold change
qRT
ELISA
Days post treatment

Fig. 5.

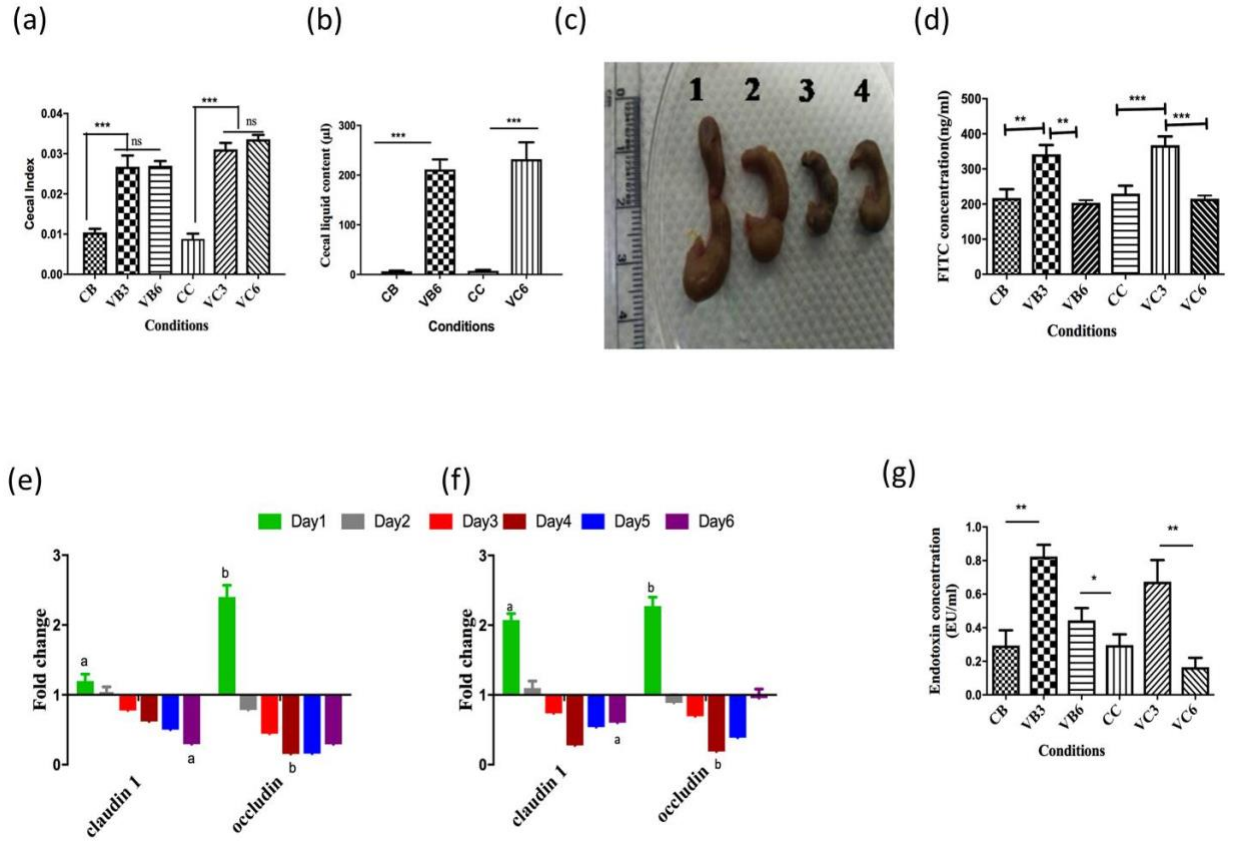
(a)
(b)
(c)
(d)
Cecal Index
Cecal liquid content (µl)
FITC concentration(ng/ml)
Conditions
CB
VB3
VB6
CC
VC3
VC6
1
2
3
4
(e)
(f)
(g)
Day1
Day2
Day3
Day4
Day5
Day6
Fold change
claudin 1
occludin
Endotoxin concentration (EU/ml)

Fig. 6.

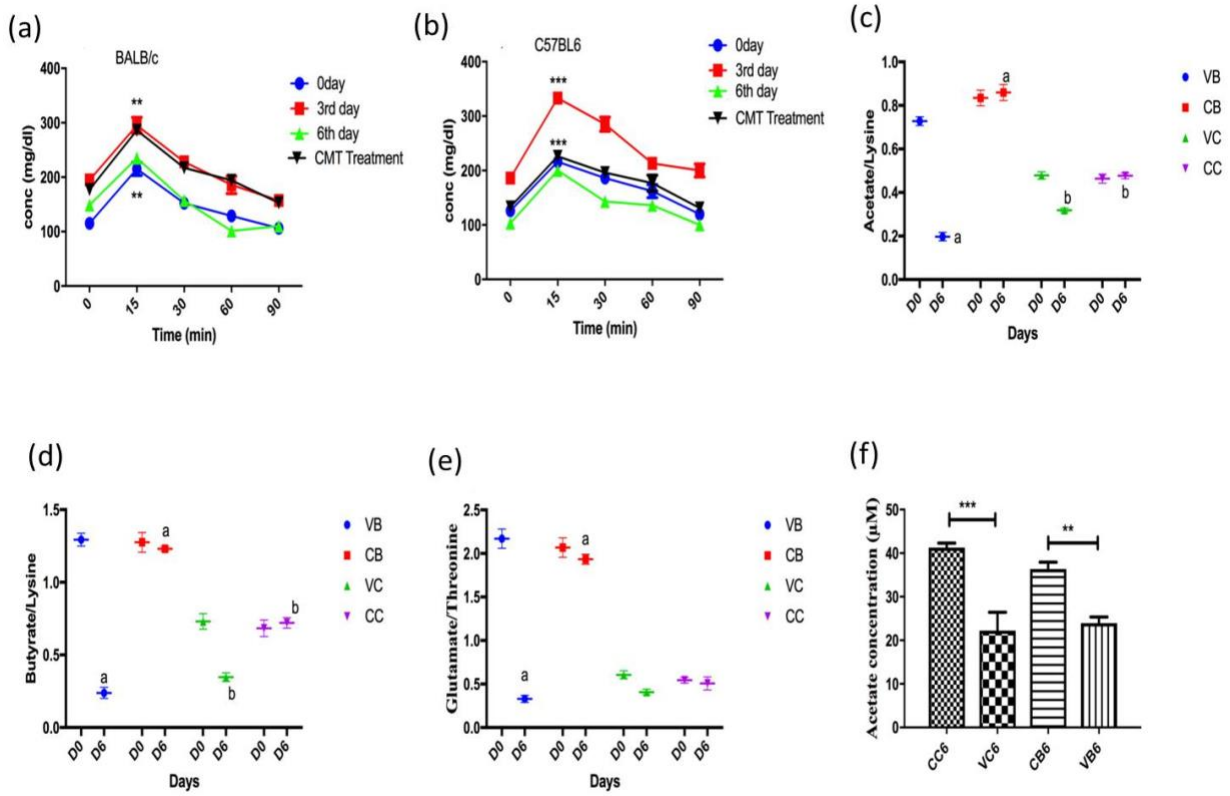
(a)
BALB/c
conc (mg/dl)
Time (min)
0day
3rd day
6th day
CMT Treatment
(b)
C57BL6
conc (mg/dl)
Time (min)
0day
3rd day
6th day
CMT Treatment
(c)
Acetate/Lysine
Days
VB
CB
VC
CC
(d)
Butyrate/Lysine
Days
VB
CB
VC
CC
(e)
Glutamate/Threonine
Days
VB
CB
VC
CC
(f)
Acetate concentration (μM)
CC6
VC6
CB6
VB6

Fig. 7.

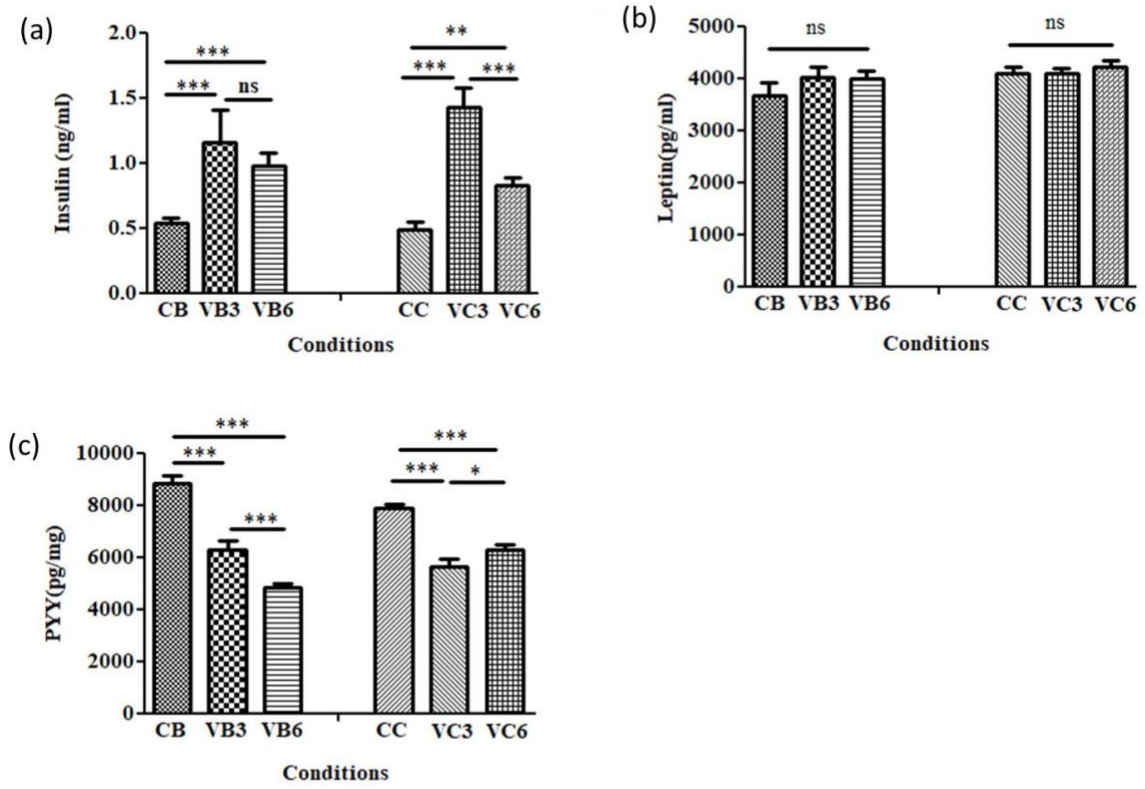
(a)
Insulin (ng/ml)
2.0
1.5
1.0
0.5
0.0
***
***
ns
**
***
***
CB VB3 VB6
CC VC3 VC6
Conditions
(b)
Leptin(pg/ml)
5000
4000
3000
2000
1000
0
ns
ns
CB VB3 VB6
CC VC3 VC6
Conditions
(c)
PYY(pg/mg)
10000
8000
6000
4000
2000
0
***
***
***
***
***
*
CB VB3 VB6
CC VC3 VC6
Conditions